Temperature dynamics and velocity scaling laws for interchange driven, warm ion plasma filaments

J.M.B. Olsen[1], J. Madsen[1], A.H. Nielsen[1], J. Juul Rasmussen[1], V. Naulin[1]

[1] *PPFE, Department of Physics, DTU, DK-2800 Kgs. Lyngby, Denmark*

Introduction

One of the major topics in magnetically confined fusion is how to control the radial transport of heat and particles from the region of closed magnetic field lines, know as the plasma core, across the last closed flux surface (LCFS) into the region of open magnetic field lines known as the scrape of layer (SOL). It is well established that the transport in the far scrape-off layer is predominantly turbulent. Previous studies[1] have shown that up to 50% of the radial transport can be attributed to dense coherent plasma filaments, also known as blobs. These blobs may reach plasma facing components (PFC) causing peak heat loads over the material limits leading to sputtering, a higher concentration of impurities, which can eventually lead to disruption.

Due to large parallel electron heat conduction, the ion temperature typically exceeds the electron temperature in the far SOL. This means that the energy transport in the far SOL is dominated by ions. Also interactions with neutrals in the form of ionisation and charge exchange are influenced by ion temperatures. However, there are very few measurements of ion temperatures and it is therefore interesting to simulate the effects of these.

We present investigations of the effects of temperature dynamics on the evolution of seeded blobs (blobs initialised as Gaussian perturbations on a constant background) in the SOL, including the effects of finite Larmor radii (FLR). Particularly we have studied how the blob transport is influenced by parameters such as blob size, σ, and ion to electron temperature ratio, τ. This has been done through numerical simulations using the 2D drift fluid model, HESEL[2, 3].

Influence of blob size and amplitude

Temperature dynamics have a significant influence on plasma blob transport. Figure 1 shows the particle density with respect to the background, n/n_0, vorticity normalised to the ion gyro-frequency, ω, electron temperature, T_e, and ion temperature, T_i, after 20 interchange times[5]. The figure shows a plane perpendicular to the magnetic field located at the outboard mid-plane of a tokamak from four different simulations. The initial parameters in all four simulations are identical, but the level of detail of the temperature dynamics is different: Case 1) no ion temperature effects and isothermal electrons. Case 2) dynamic electron temperatures, but no ion temperature effects. Case 3) dynamic electron temperatures and finite, but isothermal ion temperatures. Case 4) both dynamic electron and ion temperatures.

The most notable difference is seen in the vorticity, ω, between case 2 and 3, where the inclusion of finite ion temperatures breaks the poloidal symmetry of the blob and where the vorticity is a factor of 10 larger and elongated along the blob instead of being anti symmetric around the center. The inclusion of dynamic ion and electron temperatures only slightly changes the evolution of the blobs compared to the isothermal counterparts, seen when comparing case 1 and 2 for electrons and case 3 and 4 for ions. Dynamic electron temperatures causes the blob to spread out more and the lobes behind the blob front become more prominent. The inclusion of dynamic ion temperatures causes the blob to remain more coherent and propagate further through the SOL. Compared to the inclusion of finite ion temperatures when going from case 2 to 3, however, these differences are minor.

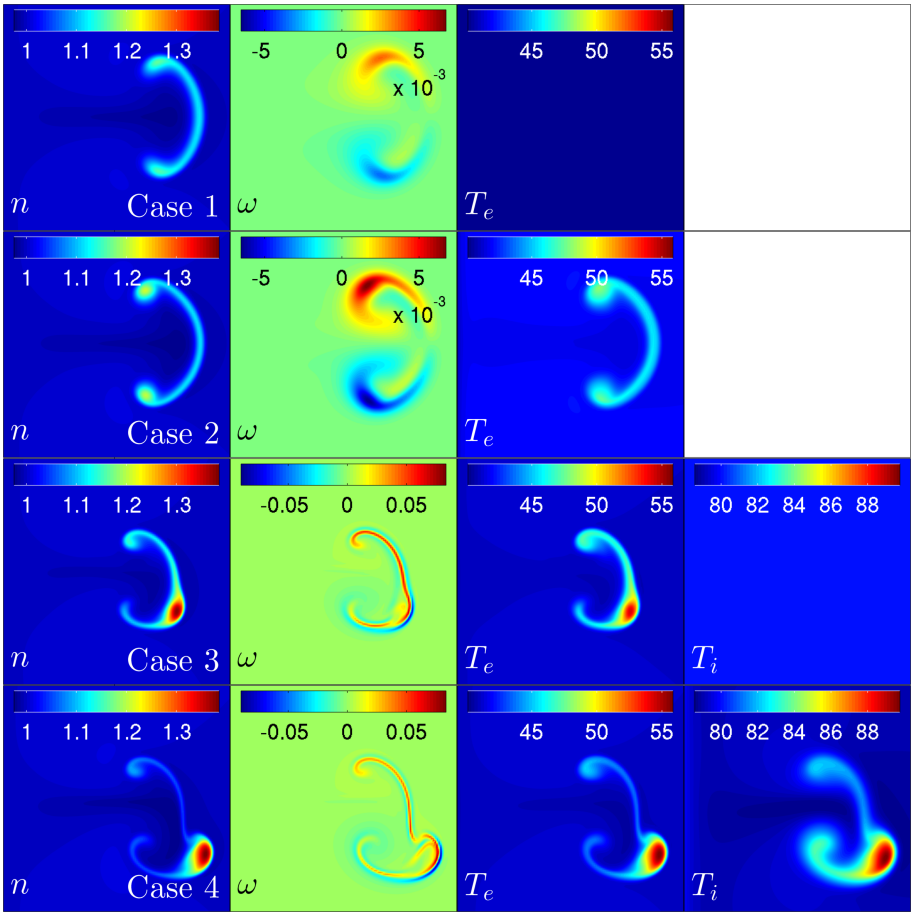

Figure 1: *Blob particle density normalised to the background density, n/n_0, vorticity, ω, electron temperature in eV, T_e and ion temperature in eV, T_i, in a plane perpendicular to the magnetic field after 20 interchange times[5]. All four simulations have the same initial parameters, but different levels of detail in the temperature dynamics. In Bohm normalised units the initial values for the blobs are: Blob width, $\sigma = 20$, ion to electron temperature ratio, $\tau = 2$, and density perturbation amplitude, $\Delta n/n_0 = 0.5$.*

Effect with initial conditions

We have observed that blobs remain more coherent with the inclusion of finite ion temperatures. The influence of the finite ion temperatures, however, varies with different initial param-

eters. The difference can be illustrated through the compactness, I_c, of the blobs defined in Ref. [4]. The compactness is a measure of how well the initial shape is retained as the blob propagates through the SOL. If $I_c = 1$, the blob completely retains its initial shape and if $I_c = 0$, the blob completely disperses.

Figure 2 shows the compactness of blobs after 15 interchange times, γ (see Ref. [5] for a thorough explanation), as a function of the parameter $r = \rho_i \Delta n/(\sigma n_0)$, which is a measure of the strength of the FLR effects[4]. Here ρ_i is the ion gyroradius. We observe an increase in the compactness between $r = 0$ and $r = 0.1$, where blobs go from dispersing rapidly to propagating through the SOL as coherent structures. Thus when the blob is subjected to strong FLR effects, it propagates further as a coherent structure through the SOL.

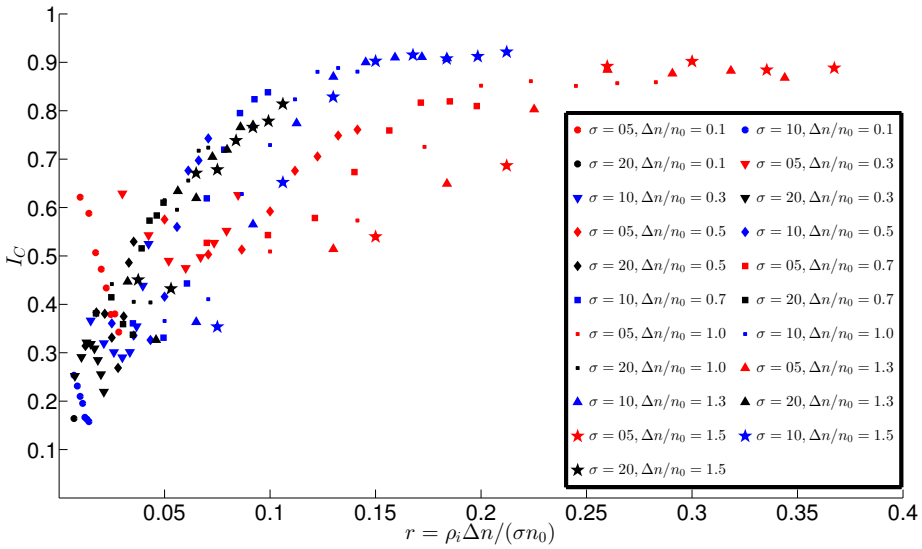

Figure 2: *Compactness, I_c, of blobs as a function of the parameter $r = \rho_i \Delta n/(\sigma n_0)$.*

Velocity scaling laws

Blob convection is influenced by numerous parameters such as size, amplitude, density, and temperature. By using dimensional analysis it is possible to deduce blob velocity scaling laws, which intend to capture the complex nonlinear dynamics in a simple expression. Here, we have investigated the validity of two scaling laws by comparison with numerical simulations. The inertial scaling law inertial scaling found in Ref. [6], here denoted as V_1, and the scaling found in Ref. [7], here denoted as V_2. The scaling laws are defined as:

$$1: \frac{V_1}{c_s} = \left(\frac{\sigma}{R} \frac{(\Delta p_e + \Delta p_i)}{p_0} \right)^{1/2}, \qquad 2: \frac{V_2}{c_s} = \sqrt{\frac{\sqrt{f^2+g^2} - f}{2}}, \tag{1}$$

where

$$f = \left(\frac{\tau \rho_s}{2\sigma} \frac{\Delta p_e}{p_0} \right)^2, \qquad \text{and} \qquad g = (1+\tau) \frac{2\sigma}{R} \frac{\Delta p_e}{p_0}, \tag{2}$$

$\Delta p_{e(i)}$ is the electron (ion) pressure perturbation, p_0 is the background pressure, R is the major radius, and c_s is the sound speed. In Figure 3 we have plotted the normalised difference between

the numerically found maximum centre of mass velocity and the two scaling laws, $\delta = (V_{max} - V_{(1,2)})/V_{(1,2)}$. So if the scaling fits perfectly, all points should lie on $\delta = 0$. Figure 3a shows δ as a function of σ. We observe that for small values of σ, scaling 1 overestimates the velocity, whereas scaling 2 underestimates it by up to a factor of 4. For large values of σ, however, both scalings slightly overestimate the velocity, but catch the overall evolution well with increasing blob size. Figure 3b shows the δ as a function of τ. We observe that both scalings overestimate the maximum velocity of the blobs, but capture the overall evolution well for blobs with large σ. Scaling 2 for blobs with small σ, however, shows a decrease in the maximum velocity with an increase in τ, which gives large deviations compared to the numerically found values.

None of the scalings thus capture the full dependence on the initial parameters within the parameters examined, but the simplest scaling, 1, appears to capture the dependence best.

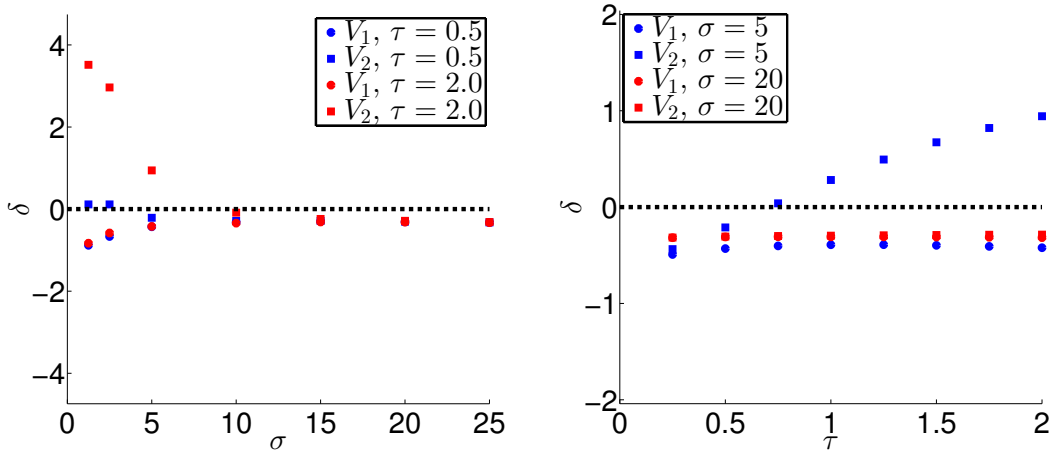

(a) δ *as a function of blob size,* σ. (b) δ *as a function of* τ.

Figure 3: *Normalised maximum velocity difference as a function of initial parameters.*

Acknowledgements

This work has been carried out within the framework of the EUROfusion Consortium and has received funding from the Euratom research and training programme 2014-2018 under grant agreement No. 633053. The views and opinions expressed herein do not necessarily reflect those of the European Commission.

References

[1] J.A. Boedo et. al., Phys. Plasmas **10**, 5 (2003)

[2] J. Madsen et. al., Phys. Plasmas **23**, 032306 (2016)

[3] A.H. Nielsen et. al., Phys. Lett. A. **379**, 3097-3101 (2015)

[4] J. Madsen et. al, Phys. Plasmas **18**, 11 (2011)

[5] J. Olsen et. al, Plasma Phys. Control. Fusion **56**, 044011 (2016)

[6] R. Kube, O.E.Garcia, Phys. Plasmas **18**, 10 (2011)

[7] P. Manz et. al, Phys. Plasmas **20**, 10 (2013)